PCCP

REVIEW

View Article Online
View Journal | View Issue

Cite this: *Phys. Chem. Chem. Phys.*, 2023, **25**, 15085

Solid-state emitters presenting a modular excited-state proton transfer (ESIPT) process: recent advances in dual-state emission and lasing applications

Martyna Durko-Maciag, [a] Gilles Ulrich, [b] Denis Jacquemin, [cd] Jaroslaw Mysliwiec *[a] and Julien Massue *[b]

Received 28th February 2023,
Accepted 9th May 2023

DOI: 10.1039/d3cp00938f

rsc.li/pccp

This review aims at providing a broad readership of material and physical chemists, as well as those interested in *ab initio* calculations, about recent advances in the fields of dual solution-solid emitters and lasing applications based on organic dyes displaying an excited-state intramolecular proton transfer (ESIPT) process. ESIPT is known to be highly sensitive to the immediate environment leading to the engineering of a wide range of stimuli-responsive fluorescent dyes. With the structural diversity of ESIPT-capable fluorophores being large, many applications have been targeted over the years in the fields of optoelectronics, biology and luminescent displays. This review wishes to point out two emerging applications concerning ESIPT fluorophores, which are the answer for the quest for emitters fluorescing both in solution and in the solid state, and those capable of light amplification.

Introduction

Proton transfer is ubiquitous in nature and is at the origin of numerous biological regulation processes within living organisms but it has also been employed in molecular materials science to engineer responsive organic molecules where a signal or information can be conveyed along a π-conjugated molecular scaffold.[1] Among the various possibilities of prototropy, excited-state intramolecular proton transfer (ESIPT) consists in an ultrafast phototautomerization, on the subpicosecond scale, between a photoexcited normal (N*) isomer and its corresponding tautomeric species (T*). ESIPT is commonly observed in heterocyclic π-conjugated molecules of natural or synthetic origin, containing a strong internal hydrogen bond embedded within five- or six-membered rings.[2] While a range of proton donors and acceptors of different nature can be found in the literature, a large number of cases narrow down the ESIPT process to an enol (E*)/keto (K*) tautomery occurring upon photoexcitation. ESIPT induces a strong reorganization of the molecular geometry of dyes in the excited-state leading to a fluorescence response presenting large Stokes shifts (up to 12 000 cm^{-1}), thereby limiting reabsorption processes and subsequent inner filter effects, both of which often yield detrimental photobleaching.[3] Additionally, while the vast majority of organic fluorescent dyes are only emissive in dilute solution and not in the solid-state due to aggregation-caused quenching (ACQ) processes,[4] ESIPT fluorophores are usually faintly luminescent in solution but strongly brighten up when molecular motions are restricted. In a similar fashion, aggregation-induced emission (AIE) corresponds to the fluorescence enhancement upon restriction of molecular rotations;[5] and this increasingly popular feature can be further augmented by the introduction of ESIPT centers on the core of the AIE dyes.[6] ESIPT emitters have long been known as attractive solid-state emitters, with adaptive optical profiles depending on the environment, *e.g.* amorphous powders, crystals, and polymeric thin films or embedded in various matrices, such as nanoparticles or aggregates.[7] Indeed, another characteristic of ESIPT fluorescence lies in its strong sensitivity to the immediate environment.[8] Intramolecular prototropy can indeed compete with other processes depending on the physical nature of the environment, strongly impacting the optical properties. As a result, synthetic organic fluorophores displaying an ESIPT process have been studied with the view of benefitting from the competitive dynamics occurring between the various possible excited-states, which paves the way for the engineering of environment-responsive molecular switches (Fig. 1).[9] Indeed, as the ESIPT process is typically under thermodynamic control, one possibility is that the ultrafast population

[a] *Wroclaw University of Science and Technology, Wyspianskiego 27, 50-370 Wroclaw, Poland. E-mail: jaroslaw.mysliwiec@pwr.edu.pl*
[b] *Institut de Chimie et Procédés pour l'Energie, l'Environnement et la Santé (ICPEES), Equipe Chimie Organique pour la Biologie, les Matériaux et l'Optique (COMBO), UMR CNRS 7515, Ecole Européenne de Chimie, Polymères et Matériaux (ECPM), 25 Rue Becquerel, 67087 Strasbourg Cedex 02, France. E-mail: massue@unistra.fr*
[c] *Nantes Université, CNRS, CEISAM UMR 6230, F-44000 Nantes, France*
[d] *Institut Universitaire de France (IUF), F-75005, Paris, France*

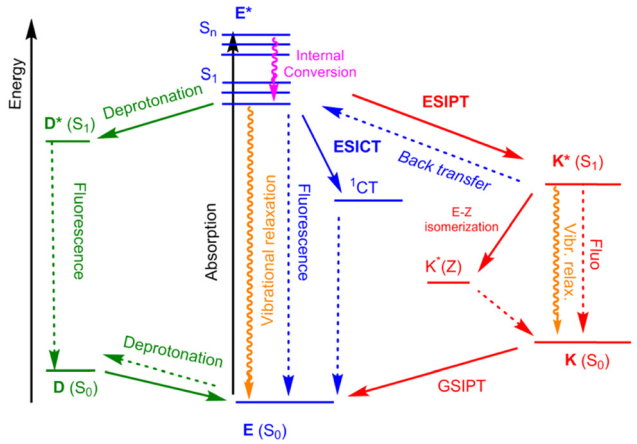

Fig. 1 Schematic representation of the ESIPT process, along with selected other competitive processes.

of K* could lead to an equilibrium with a stabilized low-lying E* state, leading to dual E*/K* emission.[10] Dual emitters with adaptable intensity ratios between emission bands are good candidates for ratiometric detection,[11] panchromatic monomolecular white fluorescence,[12] and can be applied in optoelectronics devices, as well as security cryptographic inks. Additionally, organic dyes with an intramolecular hydrogen bond and a structure showing a strong push–pull character can also trigger a competition between ESIPT and excited-state intramolecular charge transfer (ESICT) processes.[13] Finally, in dissociative media, a full or partial competition with deprotonation can also be observed, producing anionic species, some showing particularly intense fluorescence.[14] All these processes can simultaneously compete to produce fluorophores with complex emission profiles highly dependent on the polarization of their close environment (Fig. 1).[15] The literature is rich of examples of H-bonded ESIPT-capable dyes with 5-, 6-membered rings or more in their molecular backbone;[16] yet, the 2-(2′-hydroxyphenyl)benzazole (HBX, with X = NR, benzimidazole (HBI), X = O, benzoxazole (HBO) and X = S, benzothiazole (HBT)) fluorophores remain the most studied families of dyes displaying ESIPT, owing to their ease of synthesis and synthetic modification, versatility and possibility to induce drastic optical changes upon small molecular inputs.[17]

Recently, there has been global interest in the engineering of fluorophores, capable of displaying strong emission both in dilute solution and in the solid-state. This class of compounds, called dual-state emission (DSE) fluorophores or solution and solid-state emitters (SSSEs), has emerged as promising alternatives to fill the gap between the systems relying on either ACQ or AIE processes, as they allow targeting a wider range of applications in the fields of biotechnologies and optoelectronics. Several recent reviews already compiled examples and mechanisms underlying the photophysics of these compounds.[18] For all the reasons aforementioned, the ESIPT process can play a pre-eminent role not only in optimizing the DSE properties of existent dyes but also in the search of original compounds; the current challenge being the increase of fluorescence intensity in solution while maintaining strong emission quantum yield in solid. In this context, theoretical calculations appear as a tool of choice for rationalizing and understanding the properties of such compounds.

In parallel, lasing has also been proved to be an important field of application for organic dyes. Indeed, lasers stand out due to their remarkable properties, which allowed for the accelerated development of many fields, ranging from various areas of applied science, through commercially available household appliances, to medical applications.[19] In response to such a large demand for lasers, it appeared necessary to optimize and improve the properties of the devices themselves, by searching for new active organic materials capable of amplifying light and understanding the processes taking place and notably, the conditions for obtaining a population inversion. In this context, the ESIPT process due to its four-level system offers an attractive possibility to upgrade or optimize the properties of laser dyes, while offering a stronger degree of modularity. As a result, research on ESIPT-capable lasing dyes is currently very active.

This mini-review aims at updating the readers on recent advances in the two emerging fields of research (DSE dyes and organic lasing based on ESIPT fluorescence) which have seen recent remarkable developments where ESIPT-capable fluorophores lead to an improvement of technologies and can further help tackle important future challenges.

Dual-state emission

General considerations and recent examples

As mentioned in the Introduction section, DSE processes correspond to dyes showing emission both in solution and in the solid state, which can therefore target a wider range of applications than the majority of structures based on either ACQ or AIE processes that are typically not or very poorly emissive in one of the two environments. There are no identified ground rules for the elaboration of DSE materials, although a few trends have already emerged. Indeed, many DSE fluorophores arise from a combination within the same backbone of a planar aromatic core, prone to ACQ, judiciously substituted with AIE units aiming at increasing solid-state fluorescence. The DSE process is therefore obtained from a tenuous compromise between quasi-planarity, semi-rigidity, and solubility. The presence of heteroatoms on the π-conjugated scaffold of DSE dyes is also frequently observed, inducing intramolecular charge transfer (ICT) within the structures, creating dipole moments, and therefore promoting significant geometrical reorganization between the ground and excited states.

The majority of DSE fluorophores are non-ESIPT heterocyclic scaffolds, and examples can be found in several hallmark dye families, *e.g.*, triphenylamine,[20] phtalamides,[21] benzo[1,2,5]thiadiazole,[22] boron complexes,[23] and arenes.[24] As mentioned earlier, the main challenge appears to be the reduction of fluorescence quenching in solution, while maintaining solid-state emission. The key parameters to efficiently combine ESIPT and DSE seem to arise from an increase of rigidity by

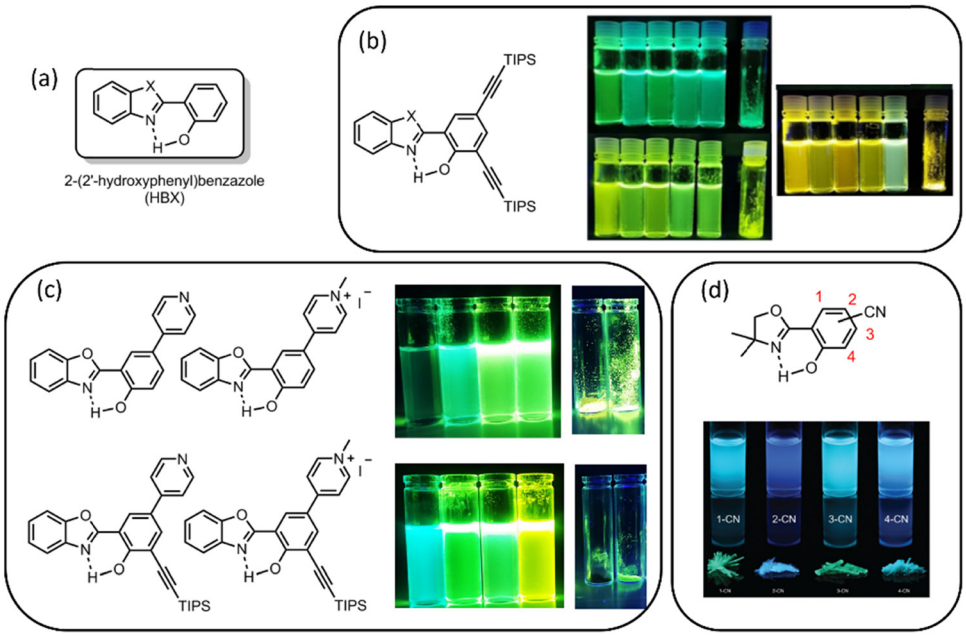

Fig. 2 Examples of the derivatization of the HBX core with (a) unsubstituted HBX dyes, (b) ethynyl-extended trialkylsilane HBX dyes (photographs correspond to HBI, HBO and HBT dyes in solution in different solvents), and (c) pyridine or pyridinium-substituted HBX dyes (solutions at the top correspond to pyridine-substituted dyes and solutions at the bottom correspond to pyridinium-substituted dyes). (d) Introduction of cyano moieties on the scaffold of phenol-oxazoline rings.[26–30] Adapted from ref. 26*b* Copyright 2021 John Wiley and Sons. Adapted from ref. 28 Copyright 2022 Elsevier. Adapted from ref. 30 Copyright 2020 the Royal Society of Chemistry.

reducing molecular motions, combined with a drastic reduction of the accessibility of the conical intersection (CI) related to the twisted intramolecular charge transfer (TICT) process often taking place after ESIPT. Obviously, the presence of a low-lying CI typically quenches fluorescence. Restricting the access to CI(s) has been proposed as a key strategy for the engineering of DSE fluorophores, by strongly diminishing the related non-radiative excited-state deactivations in solution.[25] Among the reported ESIPT-capable fluorophores, HBX dyes with DSE properties have also been reported in recent literature (Fig. 2a). Recent examples of simple derivatization of the HBX scaffold have been particularly efficient for improving solution-state fluorescence while maintaining strong quantum yield values in the solid state. Notably, a series of ethynyl-extended HBX dyes indicated a significant effect of both rigidification and delocalization at the selected position of the phenol ring (Fig. 2b).[26] Another straightforward alternative to engineer HBX with DSE properties is to introduce one or two pyridine rings. It was found to be an expedite way to reduce CI processes and restore fluorescence in solution, a feature which can be further enhanced by the formation of the corresponding pyridinium moieties (Fig. 2c).[27] The authors state that the introduction of pyridine rings favors the stabilization of a merocyanine-like species in the excited-state, strongly decreasing non-radiative deactivations. According to *ab initio* calculations, *N*-methylpyridinium was able to stabilize the K* state and subsequently disfavor non-radiative deactivations. Unfortunately, the introduction of a cationic species led to enhanced fluorescence quenching of emission in the solid state, owing to unfavorable cation–π interactions, opening non-radiative deactivation channels. Very recently, it was shown that the double introduction of both ethynyl extension and pyridine or pyridinium triggered a cooperative effect for the engineering of DSE properties (Fig. 2c).[28] Five-membered oxazoline rings are structurally analogous to benzoxazole rings, yet with a stronger degree of flexibility, and have been reported to display DSE emission. Göbel *et al.* studied the influence of electronic substitution on this minimalistic ESIPT fluorophore, notably considering strong electron-withdrawing substituents (CF_3 and CO_2Me).[29] The same team also reported nitrile-substituted 2-(oxazolinyl)-phenols where the position of the nitrile substituents induced different effects (Fig. 2d).[30]

Other examples of ESIPT/DSE dyes within the HBX family include rigidified benzimidazole derivatives, including *N*-arylated 9,10-phenanthroimidazole[31] and an example by Takagi *et al.* where the fluorescence intensity can be enhanced by the introduction of supramolecular H-bonded rigidification.[32] The same group also investigated the influence of structural rigidification by ring fusion on the optical properties of the resulting dyes.[33] Among the HBX family, benzothiazole-based derivatives (HBT) have been particularly scrutinized, due to the electron-donating nature of sulfur, leading to redshifted emission, making them better candidates for biological applications. Notably, a dual-channel fluorescent HBT probe for the logic-based visualization of aging biomarkers (thiophenol and hypochlorous acid HCOCl) was developed.[34] Moreover, Kaur *et al.* delocalized the HBT dye with a styryl spacer capable of tuning the emission color over a wide range.[35] Other organic scaffolds

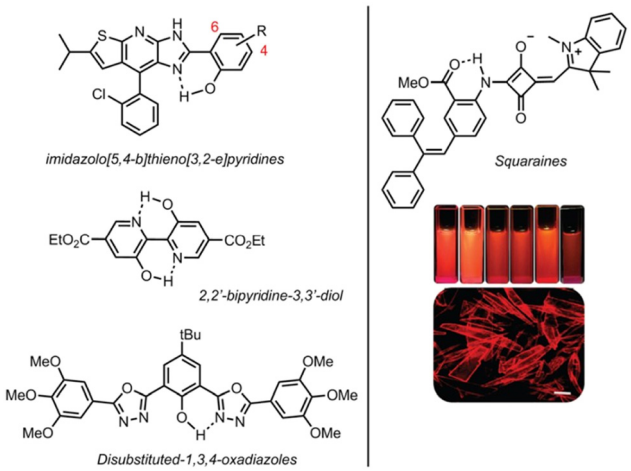

Fig. 3 Examples of miscellaneous ESIPT fluorophores showing DSE properties.[36–39] Adapted from ref. 39 Copyright 2020 the Royal Society of Chemistry.

showing both ESIPT and DSE properties can be found in the recent literature (Fig. 3). Notable examples include imidazolo-[5,4-*b*]thieno[3,2-*e*]pyridine derivatives, where the DSE properties are explained by the finely controlled self-assembly and the restriction of TICT processes.[36] A double H-bonded 2,2′-bipyridine-3,3′-diol-5,5′-dicarboxylic acid ethyl ester has been reported as a single ESIPT emitter while the other hydrogen bond participates in the rigidification of the overall scaffold, making this dye suitable for an insertion in OLED devices.[37] Other examples include 2,5-disubstituted-1,3,4-oxadiazoles[38] and most importantly red/NIR emissive squaraine derivatives.[39] Guided by TD-DFT calculations, the authors demonstrate that the removal a simple phenyl ring led to intense red/NIR emissions in solution and in crystals. A subtle alleviation of the TICT mechanism within the structure of these dyes appears to be at the origin of these attractive photophysical properties.

First-principles calculations

As for all excited-state processes relying on ultra-fast processes, theoretical modelling is often used to shed a complementary light onto the experimental results. Indeed, theory can rather straightforwardly provide some key information, such as the excited-state geometries, that typically cannot be determined using experimental approaches. For the specific case of ESIPT dyes, as illustrated by the above discussion, two specific aspects are challenging for theory: (i) the relative energies of the tautomers should be determined with high accuracy; (ii) an appropriate modelling of the environment is often required to reach valuable insights, since both the proton-transfer itself and the emission properties of the two tautomers are significantly tuned by the medium. The purpose of this section is to describe the selected examples of works that have been focused on capturing these environmental effects, which is of high relevance for DSE, so that we do not describe gas phase calculations below. For a more general discussion regarding both the theoretical methods and computational strategies that can be used to describe ESIPT dyes, we refer the interested readers to the excellent 2021 review of Jankowska and Sobolewski, who provided an overview of these approaches as well as interesting advices for appropriate modelling ESIPT in organic dyes.[40] In the next two paragraphs, we describe the methods available for the solvated and solid-state case.

For modelling ESIPT emission in solution, most works rely on the so-called continuum solvation models, and the most well-known being the polarizable continuum model (PCM) originally developed in Pisa and implemented in several popular quantum chemistry packages.[41] In continuum approaches, the environment is represented as a structureless medium having the key physical features of the actual macroscopic solvent, and such a computational strategy is very computationally effective, although it cannot accurately describe specific solute–solvent interactions, and is therefore not well-suited for protic solvents that tend to form hydrogen bonds with the ESIPT dye. For a non-protic medium, PCM and other similar models offer a generally excellent compromise between the computational efforts and the quality of the results. Various continuum models have been coupled with a wide variety of excited-state electronic structure approaches,[42] and one specific aspect needs to be addressed: the nature of the coupling between the solution and the excited-state. One can roughly split the solvent models into the linear-response and state-specific approaches.[43] The former linear-response contribution stems from the coupling between the transition dipole moment and the solvent, and the magnitude of this contribution is therefore roughly dependent on the transition probability (oscillator strength).[44] In other words, linear-response effects are large for bright transitions. The latter contributions depend on the change of polarity of the compound during the investigated electronic transition, and its magnitude is therefore roughly linked to the change of the dipole moment between the two states, *i.e.*, state-specific effects are significant for transitions involving significant charge-transfer.[45] For ESIPT dyes, the enol and keto forms have often vastly different emission signatures, and the former is both more polar and more dipole-allowed than the latter, at least in most HBX derivatives. This specific feature of ESIPT dyes motivated one of us to propose a computational protocol that includes simultaneously these linear-response and state-specific effects, an approach that is denoted as cLR^2-PCM (cLR stands for the corrected linear response).[46] A typical example of the application of this model is shown in Fig. 4 where we report keto-enol fluorescence differences for two dyes solvated in

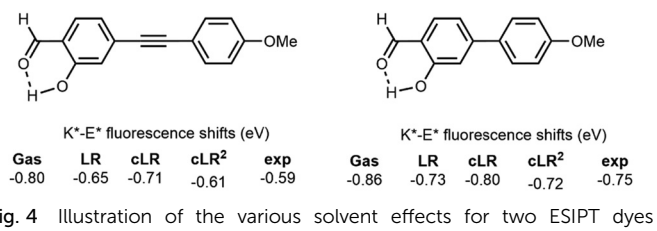

Fig. 4 Illustration of the various solvent effects for two ESIPT dyes solvated in toluene. The reported values are the difference between the K* and E* emission energies for the two displayed dyes. See ref. 46*b* for more details regarding the levels of theory used.

toluene, a solvent that would likely be considered as yielding rather mild changes as compared to gas. One nevertheless notes that the gas phase K*–E* shifts are too large as compared to the experiment. Interestingly, both the linear-response (LR) and state-specific (cLR) models do provide corrections in the expected direction, which is the logical consequence of larger corrections for the enol structure than those for the keto one. This is related to the fact that the fluorescence transition in E* is both more dipole-allowed (oscillator strength 20 times larger for the compound displayed on the left-hand side of Fig. 4) and originating from a much more polarized state (twice larger excited-state dipole for the same compounds) than its K* counterpart, inducing both large (small) linear-response and state-specific corrections for E* (K*). As can be seen for one of the two compounds, only the use of cLR[2] therefore allows reproducing the experiment in a satisfying manner, whereas both LR and cLR[2] are successful for the other, in which the charge-transfer is more limited. Of course, more refined solvation models, allowing the capturing of specific solute–solvent interactions, have been successfully applied to ESIPT as well.[47] As noted above, the emission efficiency of ESIPT HBX dyes is closely related to the accessibility of low-lying CI corresponding to the interring twisting after ESIPT took place, similar to the TICT process. This CI was originally evidenced by theoretical calculations performed in the gas phase,[48] but is now well-recognized to be the key one in both solution and in the solid-state.

Whilst the actual description of the CI itself requires using a multi-reference method that is typically too computationally demanding for large compounds, it has been suggested by some of us that one can explore the barrier separating K* from the CI using simpler approaches. To illustrate this point, we selected the calculations performed in ref. 14*a* for substituted HBO dyes and are summarized in Fig. 5. Considering the values determined in toluene, one can notice a clear correlation between the computed twisting barriers and the measured quantum yields, with the largest (smallest) calculated barrier being associated with the brightest (darkest) compound. Although this work relied on a continuum model, one can notice that the qualitative correlation pertains in ethanol. This illustrates that rather straightforward calculations can be used to qualitatively explain, and hopefully predict, some experimental trends. We nevertheless wish to close this paragraph by a word of caution: such standard TD-DFT calculations are certainly not sufficient to provide the quantitative estimates of emission yields, and one should always keep a critical eye on simplified theoretical modelling of complex phenomena.

For investigating ESIPT dyes in the solid-state, one should resort to different theoretical protocols as continuum models are generally not adequate; there are also different schemes when considering the dye in a crystalline environment or embedded in an amorphous (polymer or other) matrix. Modelling the optical properties of organic compounds in these environments is difficult; especially, for emission, yet very elegant protocols have been set up for the solid state, notably by Adamo–Ciofini[49] and Crespo-Otero teams.[50] Their approaches have in common to split the problem into the dye and its environment, with the latter being treated through a simplified quantum mechanics scheme, *i.e.*, a QM/QM′ model, in which the polarization of the QM′ environment part is self-consistently determined as a function of the excited-state density of the QM part (the dye), allowing an appropriate modeling of one of the key aspects influencing fluorescence. These approaches, or simpler ones relying on QM/MM rather than QM/QM′, have been applied to model a variety of ESIPT dyes in the solid-state.[49*a*,*b*,50*c*,51] These studies provided insights not only into the origins of the shifts of the emission band upon the changing environment, but also into the precise AIE mechanism. For instance, the authors investigated the ESIPT-able dye 2′-hydroxychalcone in its crystal state.[51*a*] This study showed that strong electrostatic interactions are detrimental for fluorescence, which is also influenced by the distortion of the crystal. It also provided insights into chemical strategies for maximizing the solid-state emission of ESIPT dyes: (i) one can stabilize E* (as compared to K*) as the non-radiative pathways are less effective in the enol form, yet this would require creating E* with a large Stokes shift; (ii) alternatively, one can hinder the access to the CI in K* by introducing fused rings preventing torsion/pyramidalization of the dye after ESIPT. In a more recent investigation performed using a large panel of high-level quantum chemical models, the same group treated a dozen of crystals built

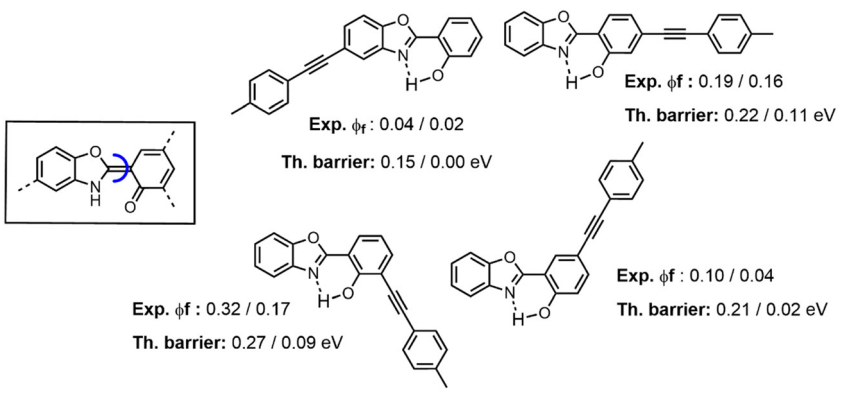

Fig. 5 Comparison between the emission quantum yields measured in solution and the computed inter-ring twisting barrier for K* from four ESIPT dyes showing DSE properties. We report data in both toluene and ethanol (Tol/EtOH). Data extracted from ref. 14*a*.

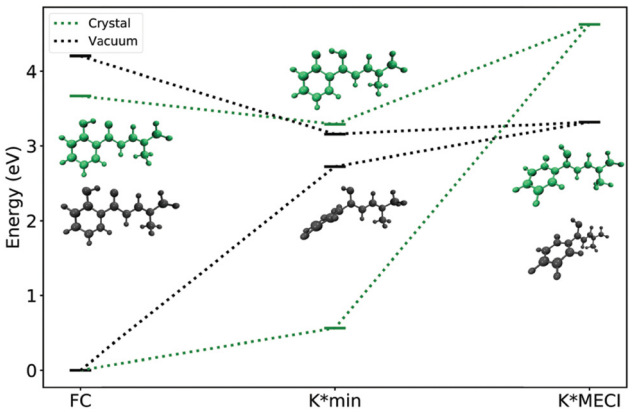

Fig. 6 Energy diagram of one ESIPT dye comparing the relative energies of the keto minimum and related CI (noted K*MECI). Reproduced from ref. 50c. Copyright 2020 the Royal Society of Chemistry. See the original work for technical details.

using ESIPT dyes and could explain all major experimental outcomes regarding the efficiency of the solid-state emission, as well as provide a series of rather generic design rules.[50c] Fig. 6, reproduced from this work, illustrates how the accessibility to the key CI discussed above strongly differs in the gas phase and in the crystal.

Lasing

Light amplification in multilevel systems

The basic two-level system consists of two energy states: ground and excited states, in which the majority of atoms of a given material are in the lowest energy state **1**, while the rest lies in the excited state **2**, according to the thermodynamic equilibrium (Fig. 7a). When we try to perform an inversion of population in such a system, which is mandatory for the LASER effect, we reach the saturation of the transition (50% of the molecules in the ground state and 50% of the molecule in the excited state) instead of the inversion, and it is not possible to obtain a lasing action.[52]

The involvement of a third energy level greatly facilitates the inversion of occupation, *i.e.*, the state in which most atoms are in an excited instead of a ground state. In this case, it is more likely that the emitted photon encounters an excited atom, leading to cascading stimulated emission instead of absorption, which can be used for the laser action. This condition is met in a three-level system where absorption results in excitation to a higher energy state **2**, followed by rapid relaxation to a metastable state **3** (Fig. 7b). If enough atoms have left the ground state **1** due to excitation, the interconversion between states **2** and **3** being fast, and state **3** has a large enough lifetime; then, the laser action occurs between states **3** and **1**. However, the continuous operation is very difficult to achieve in three-level systems, whereas it becomes highly facilitated in a four-level system, where the laser action takes place between state **3** and an additional metastable state **4**, with $E_1 < E_4 < E_3$ (Fig. 7c).

ESIPT dyes represent attractive compounds to achieve four-level systems. ESIPT materials, since the pioneering works reported by Kierstead in 1970 and Kasha in 1984,[53] have attracted much attention as the active medium necessary for the lasing action. This long interval between the two papers (14 years!) becomes understandable when looking at the first work. The laser action observed by Kierstead did not appear groundbreaking, and in addition, the species involved in the light amplification were not identified at that time. It was only when Kasha combined the laser action with the ESIPT photocycle of 3-hydroxyflavone that researchers' attention was drawn in that direction. A significant increase of interest in the following years arose from the comparison between the ESIPT four-level photocycle and the four-level of laser systems (Fig. 7c). In the ESIPT, after pumping, the excited molecule undergoes a very rapid tautomerization to the T* form, which relaxes through radiative pathways and returns to the ground state (N), allowing the N form to be re-excited. The fast kinetics of N* → T* and T → N tautomerization corresponds to the non-radiative deactivations from higher excited states in the four-level laser system (**2** → **3**, **4** → **1**), while the energy levels of the N and T forms correspond to the relevant states taking part in the laser action. As the tautomer is unstable when relaxed (state T), its population is obviously zero, which allows for the laser action between the excited and the ground levels. For this reason, ESIPT compounds can be regarded as *natural-born* materials for lasing.[54]

A short history of ESIPT-based lasers

From a historical point of view, the vast majority of the ESIPT-related light amplification investigations were focused on

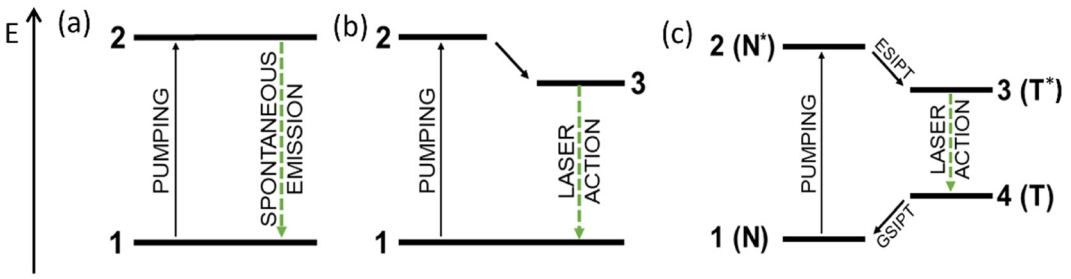

Fig. 7 (a) Two-, (b) three- and (c) four-level laser systems and ESIPT photocycle: N – normal and T – tautomer. Pumping corresponds to the excitation process. GSIPT = ground-state intramolecular proton transfer.

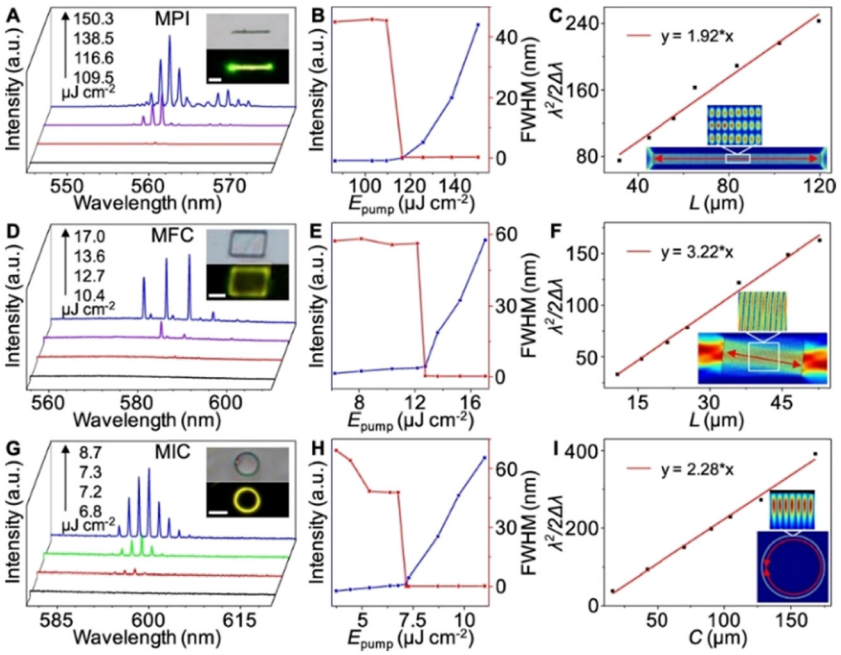

Fig. 8 Optically pumped lasing measurements. (A, D and G) PL spectra of a single MPI wire (A), MFC plate (D), and MIC ring (G) pumped at different energies. Insets: bright-field and PL images of a single wire, plate, and ring. Scale bars are 20, 5, and 20 μm. (B, E and H) Power-dependent profiles of the PL intensities (blue) and FWHM (red) of the MPI (B), MFC (E), and MIC (H). (C, F and I) Plots and fitted curves of $\lambda 2/2\Delta\lambda$ (λ = 559 nm) *vs.* the length of the MPI wires (C), $\lambda 2/2\Delta\lambda$ (λ = 581 nm) *vs.* the length of the MFC plates (F) and $\lambda 2/\pi\Delta\lambda$ (λ = 594 nm) *vs.* the circumference of the rings (I). Insets: simulated electric field intensity distributions in the wire, plate, and ring cavity.[76] Reprinted with permission from ref. 76. Copyright 2018 American Chemical Society.

developing new materials and their amplified spontaneous emission (ASE) properties in solution or in the solid-state, as reviewed by Liao in 2020.[55] As in the aforementioned works by Kasha and Kierstead, the first experiments were conducted on concentrated solutions contained in specifically designed cells, which worked as the cavity. Out of many ESIPT-type chromophores, some molecular scaffolds exhibiting great performance in light amplification can be highlighted: 3-hydroxyflavones (3-HF),[53,56–58] salicylates,[52,59,60] 2-(2-hydroxyphenyl)imidazole (HPI),[61–63] 2-hydroxychalcone[64–66] and notable HBX derivatives.[67–69] The latter, when substituted with fluorine, was used as a dopant in polymeric thin films, leading to the first observation of the solid-state lasing action from an ESIPT dye.[70] This pioneering work was followed by numerous contributions on the application of ESIPT compounds either as dopants or as crystals.[71,72]

Solid-state emission, amplified spontaneous emission, and lasing

While the four-level system of ESIPT luminescence is clearly very advantageous for the laser action, ESIPT dyes are also investigated as environment-responsive sensors due to their inherent and sensitive intramolecular hydrogen bonds.[7a,b,9b] Their optical profiles can be fine-tuned with various external stimuli, such as temperature, electrical current, humidity and environmental polarity variations.[73,74] Hence, besides the well-known spectral properties–chemical structure modifications, other paths for emission manipulation are open, *e.g.*, through co-crystal formation, as shown by Lin *et al.*,[75] leading to E*/K* emission tuning in the solid-state. They did not investigate the light amplification phenomena; but nonetheless, organic structures obtained in such a way can still be applied in lasing. A prime example can be made on co-crystal lasers,[76] which were

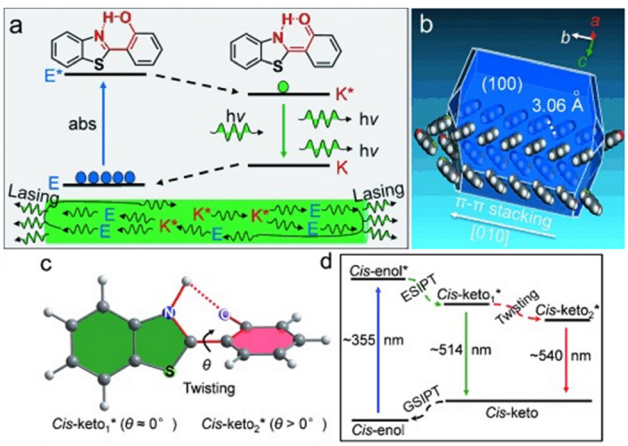

Fig. 9 (a) Illustration of the ESIPT four-level gain process based on the enol–keto phototautomerization of a model compound HBT. (b) Theoretically predicted growth morphology of a HBT crystal based on the attachment energies calculated using the Material Studio package. The predicted growth thermodynamic stable morphology is the 1D wire-like structure growing along the *b* axis. (c) Planar (*cis*-keto$_1$*) and twisted (*cis*-keto$_2$*) keto excited states. θ is the twist angle between the benzothiazole ring and the hydroxyphenyl ring. (d) ESIPT photocycle in the HBT nanowires with two *cis*-keto* states.[69] Adapted with permission from ref. 69. Copyright 2015. John Wiley and Sons.

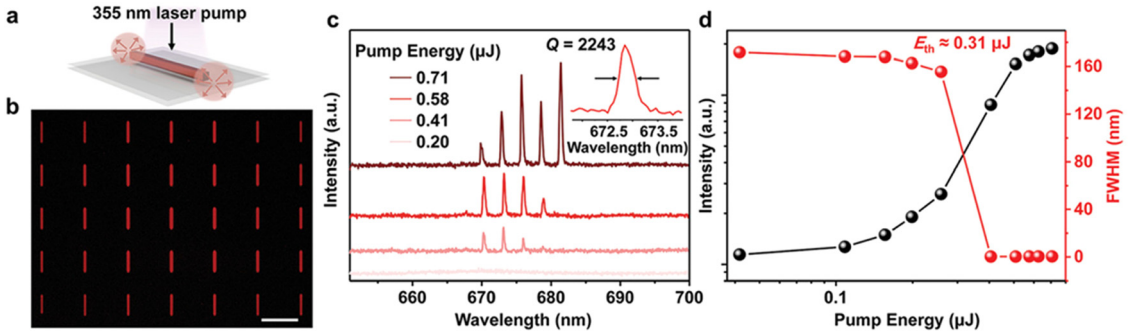

Fig. 10 Lasing performance of 1D 1,5-DHAQ single-crystalline arrays. (a) Schematic diagram of the Fabry–Pérot cavity in an organic microwire excited using a 355 nm pulsed laser beam. (b) Fluorescence microscopy image of assembled organic 1D arrays with a length of 30 μm. (c) PL spectra using an individual organic microwire with a *L* of 30 μm, which was excited at different pump energies from 0.20 to 0.71 μJ. Right inset: the zoom-in PL spectrum of the organic microwire excited at 0.71 μJ. (d) Pumping energy dependent plots of integrated intensities (black balls) and FWHM (red balls). Scale bar: (b) 50 μm.[78] Reprinted with permission from ref. 78. Copyright 2022. John Wiley and Sons.

designed as halogen acceptor–donor pairs. Chu *et al.* reported tuning of the lasing action through a change of the halogen donor, which resulted in the precise tailoring of the energy levels, and subsequent cavity structures. An ESIPT type molecule served as the acceptor, making it possible to obtain lasing of Fabry–Perot or Whispering Gallery Mode (WGM) types (Fig. 8).

Wire-like structures are often investigated in organic-based lasers, and as such one-dimensional construction can act as a Fabry–Perot resonator.[77,78] One of the most notable works evidenced wavelength-switchable lasers based on a HBT dye microwire.[69] Such a feature was accomplished through the photoisomerization of the HBT molecule: depending on the conformation of either 514 or 537 nm single-mode laser lines were obtained for planar and twister *cis*-keto forms, respectively (Fig. 9). A molecule derived from HBT was also investigated as a dopant in the 5CB matrix, and as a precursor for a novel liquid crystal.[77] The liquid crystals' ability was exploited to orient the molecules with an external electric field, which was combined with the inherent light amplification affinity of the ESIPT chromophore. Hence, it was possible to modulate the ASE behavior electrically.

The crystallization has a major impact on the lasing properties of organic compounds. 1,5-Dihydroxyanthraquinone (1,5-DHAQ) tends to form aggregates exhibiting four overlapping bands in the emission spectrum, corresponding to the fluorescence of N* and T* forms.[78,79] Single crystals obtained from this compound exhibit a square-like morphology of high quality, making it possible to apply them as WGM cavities. The same compound was also investigated as 1D arrays with controlled geometry,[78] leading to deep-red lasers of a high quality factor ($Q > 2200$) and low lasing thresholds (Fig. 10), which can, in addition, serve as vapor sensors or waveguides.

No sensing ability with these arrays during the lasing action was mentioned, even though such development could likely be the next step, as the involvement of light amplification in detection has several advantages compared to the conventional one based on spectrometric methods, *e.g.* the obtained signal has a better signal-to-noise ratio – thus a higher resolution, and the device sensitivity is also much higher. In 2016, another group investigated a different HPI-based ESIPT molecule,[63] which was also proven to work as a colorimetric vapor sensor. The interaction of alcohol vapors with the compound during the crystallization process led to five distinct crystal forms, varying in fluorescence intensity and position of the maximum wavelength. One of these structures was investigated as a potential active material for laser applications; the C1 was found to exhibit an ASE phenomenon, with an emission maximum located at *ca.* 500 nm (Fig. 11).

Emission tuning of the ESIPT process in the solid-state can also be achieved by exploiting the polymorphic abilities of these materials, analogous to organic ICT compounds,[80,81] and this was already presented on the 1-hydroxy-2-acetonaphthone derivative.[82] In 2016, Cheng *et al.* investigated hydroxyphenyl-based

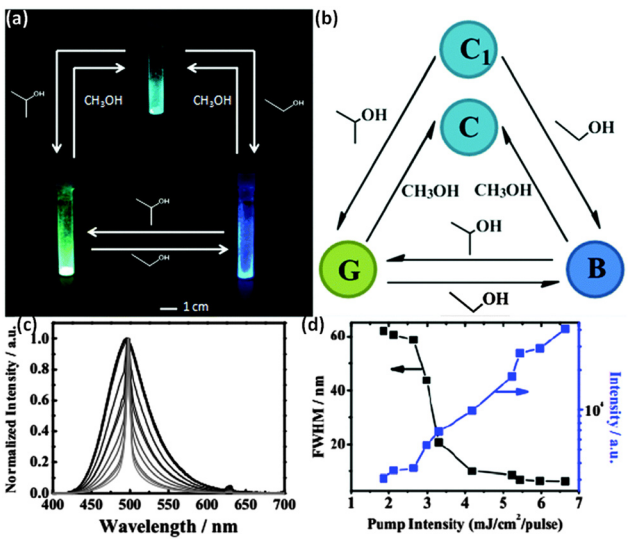

Fig. 11 (a) Photograph of the luminescence tuning cycle by three alcohol vapors. (b) Schematic illustration of the crystal changing process of H_2hpi_2cf during fluorescence color tuning based on the PXRD patterns. (c) PL spectra as a function of the pump laser energy. (d) Dependence of the peak intensity and FWHM of emission spectra of the C1-form crystal.[63] Adapted from ref. 63. Copyright 2016 the Royal Society of Chemistry.

compounds,[80] which could crystallize into two polymorphs: 1 R and 1 O. The former exhibited emission in the NIR region, whereas for its counterpart, the spectrum was significantly blueshifted. The 1 O showed not only affinity towards protonation (when crystallized with hydrochloric acid), but also predisposition to temperature-induced polymorphism. Hence, three forms of the single compound were obtained and successfully used in ASE experiments.

Efficient light confinement in the crystals made it possible to obtain stimulated emissions at 612, 650, and 714 nm

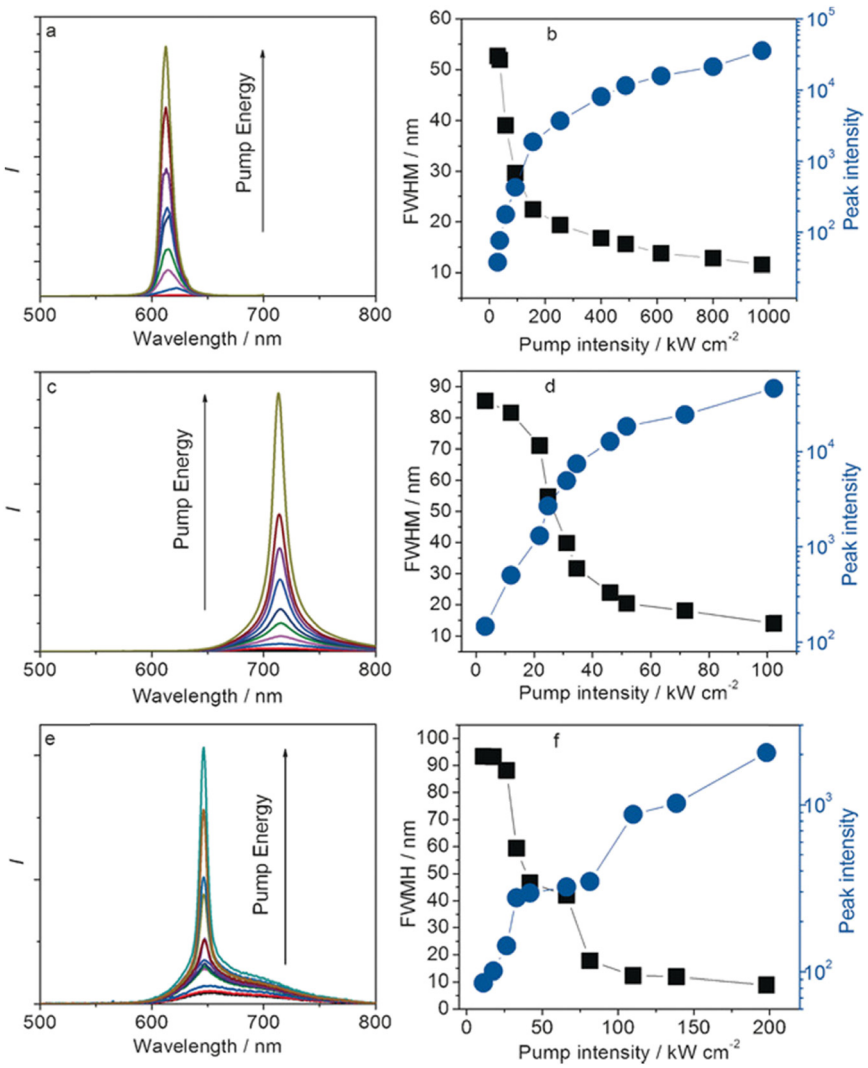

Fig. 12 (a, c and e) PL spectra as a function of the pump laser energy and the dependence of the peak intensity and (b, d and f) FWHM of the emission spectra of 1 O (a and b), 1 R (c and d) and heated 1 O (e and f). The crystal sizes are about 0.5 mm × 1 mm × 0.8 μm (1 O), 3 mm × 2 mm × 0.03 mm (1 R), and 0.5 mm × 1 mm × 0.8 μm (heated 1 O).[80] Reprinted with permission from ref. 80. Copyright 2016. John Wiley and Sons.

Table 1 Summary of the lasing properties of exemplary ESIPT-based devices

Material	Resonator	Shape	Pumping conditions	λ_{em} [nm]	Threshold	Q value	Ref.
H_2hpi_2cf (C1)	ASE	Disk	355 nm, ns	500	600 kW cm^{-2}	—	63
HBT	FP	Wire	355 nm, fs	514	197 nJ cm^{-2}	1500	66
MPI:F4DIB	FP	Plate	400 nm, fs	580	12.74 μJ cm^{-2}	1800	76
MPI	FP	Wire	400 nm, fs	560	116.5 μJ cm^{-2}	2300	76
MPI:IFB	WGM	Ring	400 nm, fs	600	7.1 μJ cm^{-2}	4500	76
C_5Ph-HBT/5CB	ASE	LC blend	355 nm, ns	557	20 mJ cm^{-2}	—	77
1,5-DHAQ	FP	Wire	355 nm, ns	673	0.31 μJ	2243	78
1,5-DHAQ	WGM	Disk	355 nm, ns	672	0.39 μJ	2033	79
1O	ASE	Crystal	355 nm, ns	612	37.1 kW cm^{-2}	—	80
Heated-1O	ASE	Crystal	355 nm, ns	653	26.4 kW cm^{-2}	—	80
1R	ASE	Crystal	355 nm, ns	714	20.8 kW cm^{-2}	—	80

(for 1 O, 1 O – heated, and 1 R, respectively – Fig. 12). Moreover, the emission of heated 1 O shifted towards shorter wavelengths upon grinding. All forms were capable of proton transfer in the excited state, ensuring a four-level system when applied in light amplification devices.

Information about solid-state ESIPT emitters for light amplification is presented in Table 1.

Conclusions and future perspectives

In conclusion, it is relatively clear that papers published in the last few years show newly emerging research trends for ESIPT compounds, not only showing intense fluorescence emission in multiple environments on the one hand but also acting as an organic laser on the other hand. For the former, *ab initio* calculations appear as indispensable tools for the rationalization of the experimental results and the elaboration of future dyes. For the latter, the characteristic four-level photocycle of the ESIPT process is a positive addition, but currently work is underway to engineer spectrally tunable emission in real-time, which could in turn affect the intensity ratio of N*/T* tautomers. The fact of being able to tune the stimulated emission in real-time will be very significant for the development of organic lasers, increasing their competitiveness compared to their widely used inorganic counterparts. Moreover, the innate sensory abilities of ESIPT dyes may be one possible way of implementing such devices, since to the best our knowledge, the possibility of obtaining stimulated emission has not been successfully applied in sensing. Such an application would be highly desired, as such devices would be characterized by high resolution sensitivity. On the other hand, panchromatic lasers are another possibility. As it was shown, desired stimulated emission spectra can be quite easily engineered, making it possible to fit the properties of the final device to the desired application. White emission and the corresponding Li-Fi (light fidelity) implementation can be highlighted in this regard. The Li-Fi systems, which utilize light to transmit data and position between devices, are based on the idea of white light emission with the utilization of LEDs as a medium. This technology is now the subject of extensive research and testing.

Similarly, ESIPT dyes can be used in bioimaging, since many of these compounds, such as salicylic acid, are biocompatible and non-toxic. Appropriate modification of the chemical structure of the dyes makes it possible to adjust the properties of these compounds so that they fit the target application, *e.g.* emission in the biological window.

Conflicts of interest

There are no conflicts to declare.

References

1 N. Amdursky, Y. Lin, N. Aho and G. Groenhof, Exploring fast proton transfer events associated with lateral proton diffusion on the surface of membranes, *Proc. Natl. Acad. Sci. U. S. A.*, 2019, **116**, 2443–2451.

2 (*a*) J. Zhao, S. Ji, Y. Chen, H. Guo and P. Yang, Excited state intramolecular proton transfer (ESIPT): from principal photophysics to the development of new chromophores and applications in fluorescent molecular probes and luminescent materials, *Phys. Chem. Chem. Phys.*, 2012, **14**, 8803–8817; (*b*) C. L. Chen, Y. T. Chen, A. P. Demchenko and P. T. Chou, Amino proton donors in excited-state intramolecular proton-transfer reactions, *Nat. Chem. Rev.*, 2018, **2**, 131–143.

3 N. N. M. Y. Chan, A. Idris, Z. H. Z. Abidin, H. A. Tajuddina and Z. Abdullah, White light employing luminescent engineered large (mega) Stokes shift molecules: a review, *RSC Adv.*, 2021, **11**, 13409–13444.

4 (*a*) T. Förster, Excimers, *Angew. Chem. Int. Ed.*, 1969, **8**(5), 333–343; (*b*) M. Tasior, D. Kim, S. Singha, M. Krzeszewski, K. H. Ahn and D. T. Gryko, π-Expanded coumarins: synthesis, optical properties and applications, *J. Mater. Chem. C*, 2015, **3**, 1421–1446.

5 (*a*) J. Mei, N. L. Leung, R. T. Kwok, J. W. Lam and B. Z. Tang, Aggregation-induced emission: Together we shine, united we soar!, *Chem. Rev.*, 2015, **115**, 11718–11940; (*b*) Z. Zhao, H. Zhang, J. W. Y. Lam and B. Z. Tang, Aggregation-induced emission: New vistas at the aggregate level, *Angew. Chem., Int. Ed*, 2020, **59**, 9888–9907.

6 (*a*) J. Jiang, H. Sun, Y. Hu, G. Lu, J. Cui and J. Hao, AIE + ESIPT activity-based NIR Cu2+ sensor with dye participated binding strategy, *Chem. Commun.*, 2021, **57**, 7685–7688; (*b*) R. Long, C. Tang, Z. Yang, Q. Fu, J. Xu, C. Tong, S. Shi, Y. Guo and D. Wang, A natural hyperoside based novel light-up fluorescent probe with AIE and ESIPT characteristics for on-site and long-term imaging of β-galactosidase in living cells, *J. Mater. Chem. C*, 2020, **8**, 11860–11865; (*c*) T. Stoerkler, P. Retailleau, D. Jacquemin, G. Ulrich and J. Massue, Heteroaryl-Substituted bis-Anils: Aggregation-Induced Emission (AIE) Derivatives with Tunable ESIPT Emission Color and pH Sensitivity, *Chem. – Eur. J.*, 2023, **29**, e202203766.

7 (*a*) V. S. Padalkar and S. Seki, Excited-state intramolecular proton-transfer (ESIPT)-inspired solid state emitters, *Chem. Soc. Rev.*, 2016, **45**, 169–202; (*b*) L. Chen, P. Y. Fu, H. P. Wang and M. Pan, Excited-state intramolecular proton transfer (ESIPT) for optical sensing in solid state, *Adv. Opt. Mater.*, 2021, **9**(23), 2001952; (*c*) M. K. Bera, P. Pal and S. Malik, Solid-state emissive organic chromophores: design, strategy and building blocks, *J. Mater. Chem. C*, 2020, **8**, 788–802.

8 J. Massue, D. Jacquemin and G. Ulrich, Molecular engineering of excited-state intramolecular proton transfer (ESIPT) dual and triple emitters, *Chem. Lett.*, 2018, **47**(9), 1083–1089.

9 (*a*) P. Gayathri, M. Pannipara, A. G. Al-Sehemi and S. P. Anthony, Recent advances in excited state intramolecular proton transfer mechanism-based solid state fluorescent materials and stimuli-responsive fluorescence switching, *CrystEngComm*, 2021, **23**, 3771–3789; (*b*) A. C. Sedgwick, L. Wu, H. H. Han, S. D. Bull, X. P. He, T. D. James,

J. L. Sessler, B. Z. Tang and H. Tian, J. Yoon. Excited-state intramolecular proton-transfer (ESIPT) based fluorescence sensors and imaging agents, *Chem. Soc. Rev.*, 2018, **47**, 8842–8880.

10 (*a*) E. Heyer, K. Benelhadj, S. Budzák, D. Jacquemin, J. Massue and G. Ulrich, On the fine-tuning of the excited-state intramolecular proton transfer (ESIPT) process in 2-(2′-Hydroxybenzofuran)benzazole (HBBX) dyes, *Chem. – Eur. J.*, 2017, **23**, 7324–7336; (*b*) S. K. Behera, S. Y. Park and J. Gierschner, Dual emission: Classes, mechanisms, and conditions, *Angew. Chem., Int. Ed.*, 2021, **60**(42), 22624–22638; (*c*) C. Azarias, S. Budzak, A. D. Laurent, G. Ulrich and D. Jacquemin, Tuning ESIPT fluorophores into dual emitters, *Chem. Sci.*, 2016, **120**, 3763–3774.

11 (*a*) T. Pariat, P. M. Vérité, D. Jacquemin, J. Massue and G. Ulrich, 2,2-Dipicolylamino substituted 2-(2′-hydroxybenzofuranyl) benzoxazole (HBBO) derivative: Towards ratiometric sensing of divalent zinc cations, *Dyes Pigm.*, 2021, **190**, 109338; (*b*) L. Wu, Y. Wang, M. Weber, L. Liu, A. C. Sedgwick, S. D. Bull, C. Huang and T. D. James, ESIPT-based ratiometric fluorescence probe for the intracellular imaging of peroxynitrite, *Chem. Commun.*, 2018, **54**, 9953–9956; (*c*) G. Zeng, Z. Liang, X. Jiang, T. Quan and T. Chen, An ESIPT-dependent AIE fluorophore based on HBT derivative: substituent positional impact on aggregated luminescence and its application for hydrogen peroxide detection, *Chem. – Eur. J.*, 2022, **28**(5), e202103241; (*d*) L. Wu, L. Liu, H.-H. Han, X. Tian, M. L. Odyniec, L. Feng, A. C. Sedgwick, X.-P. He, S. D. Bull and T. D. James, ESIPT-based fluorescence probe for the ratiometric detection of superoxide, *New J. Chem.*, 2019, **43**, 2875–2877.

12 (*a*) S. Kundu, B. Sk, P. Pallavi, A. Giri and A. Patra, Molecular engineering approaches towards all-organic white light emitting materials, *Chem. – Eur. J.*, 2020, **26**(25), 5557–5582; (*b*) K. Benelhadj, W. Muzuzu, J. Massue, P. Retailleau, A. Charaf-Eddin, A. D. Laurent, D. Jacquemin, G. Ulrich and R. Ziessel, White emitters by tuning the excited-state intramolecular proton-transfer fluorescence emission in 2-(2′-Hydroxybenzofuran)benzoxazole Dyes, *Chem. – Eur. J.*, 2014, **20**, 12843–12857.

13 (*a*) A. P. Demchenko, K.-C. Tang and P.-T. Chou, Excited-state proton coupled charge transfer modulated by molecular structure and media polarization, *Chem. Soc. Rev.*, 2013, **42**, 1379–1408; (*b*) M. Munch, E. Colombain, T. Stoerkler, P. M. Vérité, D. Jacquemin, G. Ulrich and J. Massue., Blue-emitting 2-(2′-Hydroxyphenyl)benzazole fluorophores by modulation of excited-state intramolecular proton transfer: Spectroscopic studies and theoretical calculations, *J. Phys. Chem. B*, 2022, **126**, 2108–2118; (*c*) M. Raoui, J. Massue, C. Azarias, D. Jacquemin and G. Ulrich, Highly fluorescent extended 2-(2′-hydroxyphenyl)benzazole dyes: synthesis, optical properties and first-principle calculations, *Chem. Commun.*, 2016, **52**(59), 9216–9219.

14 (*a*) M. Munch, M. Curtil, P. M. Vérité, D. Jacquemin, J. Massue and G. Ulrich, Ethynyl-tolyl extended 2-(2′-Hydroxyphenyl)benzoxazole Dyes: Solution and solid-state excited-state intramolecular proton transfer (ESIPT) Emitters, *Eur. J. Org. Chem.*, 2019, 1134–1144; (*b*) K. I. Sakai, T. Ishikawa and T. Akutagawa, A blue-white-yellow color-tunable excited state intramolecular proton transfer (ESIPT) fluorophore: sensitivity to polar-nonpolar solvent ratios, *J. Mater. Chem. C*, 2013, **1**(47), 7866–7871.

15 T. Stoerkler, D. Frath, D. Jacquemin, J. Massue and G. Ulrich, Dual-State Emissive π-Extended Salicylaldehyde Fluorophores: Synthesis, Photophysical Properties and First-Principle Calculations, *Eur. J. Org. Chem.*, 2021, 3726–3736.

16 (*a*) K. Skonieczny, J. Yoo, J. M. Larsen, E. M. Espinoza, M. Barbasiewicz, V. I. Vullev, C.-H. Lee and D. T. Gryko, How To Reach Intense Luminescence for Compounds Capable of Excited-State Intramolecular Proton Transfer?, *Chem. – Eur. J.*, 2016, **22**, 7485–7496; (*b*) M. Zhang, R. Cheng, J. Lan, H. Zhang, L. Yan, X. Pu, Z. Huang, D. Wu and J. You, Oxidative C-H/C-H Cross-Coupling of [1,2,4]Triazolo[1,5-a]pyrimidines with Indoles and Pyrroles: Discovering Excited-State Intramolecular Proton Transfer (ESIPT) Fluorophores, *Org. Lett.*, 2019, **21**, 4058–4062.

17 (*a*) Y. Chen, Y. Fang, H. Gu, J. Qiang, H. Li, J. Fan, J. Cao, F. Wang, S. Lu and X. Chen, Color-Tunable and ESIPT-Inspired Solid Fluorophores Based on Benzothiazole Derivatives: Aggregation-Induced Emission, Strong Solvatochromic Effect, and White Light Emission, *ACS Appl. Mater. Interfaces*, 2020, **12**, 55094–55106; (*b*) V. R. Mishra, C. W. Ghanavatkar and N. Sekar, Towards NIR-Active Hydroxybenzazole (HBX)-Based ESIPT Motifs: A Recent Research Trend, *ChemistrySelect*, 2020, **5**, 2103–2113; (*c*) D. Yao, S. Zhao, J. Guo, Z. Zhang, H. Zhang, Y. Liu and Y. Wang, Hydroxyphenyl-benzothiazole based full color organic emitting materials generated by facile molecular modification, *J. Mater. Chem.*, 2011, **21**, 3568–3570.

18 (*a*) T. Stoerkler, T. Pariat, A. D. Laurent, D. Jacquemin, G. Ulrich and J. Massue, Excited-State Intramolecular Proton Transfer Dyes with Dual-State Emission Properties: Concept, Examples and Applications, *Molecules*, 2022, **27**, 2443; (*b*) J. L. Belmonte-Vazquez, Y. A. Amador-Sanchez, L. A. Rodriguez-Cortes and B. Rodriguez-Molina, Dual-State Emission (DSE) in Organic Fluorophores: Design and Applications, *Chem. Mater.*, 2021, **33**, 7160–7184; (*c*) A. Huber, J. Dubbert and T. D. Scherz, J. Voskuhl. Design Concepts for Solution and Solid-State Emitters–A Modern-View point on Classical and Non-Classical Approaches, *Chem. – Eur. J.*, 2023, **29**, e2022024.

19 I. D. W. Samuel and G. A. Turnbull, Organic Semiconductor Lasers, *Chem. Rev.*, 2007, **107**, 1272–1295.

20 L. Zou, S. Guo, H. Lv, F. Chen, L. Wei, Y. Gong, Y. Liu and C. Wei, Molecular design for organic luminogens with efficient emission in solution and solid-state, *Dyes Pigm.*, 2022, **198**, 109958.

21 N. Venkatramaiah, G. D. Kumar, Y. Chandrasekaran, R. Ganduri and S. Patil, Efficient Blue and Yellow Organic Light-Emitting Diodes Enabled by Aggregation-Induced Emission, *ACS Appl. Mater. Interfaces*, 2018, **10**, 3838–3847.

22 Y. Xu, L. Ren, D. Dang, Y. Zhi, X. Wang and L. Meng, A Strategy of ''Self-Isolated Enhanced Emission'' to Achieve Highly Emissive Dual-State Emission for Organic Luminescent Materials, *Chem. – Eur. J.*, 2018, **24**(41), 10383–10389.

23 K. Ohno, F. Narita, H. Yokobori, N. Iiduka, T. Sugaya, A. Nagasawa and T. Fujihara, Substituent effect on emission of flavonolate-boron difluoride complexes: The role of π-system for dual-state (solution and solid) emission, *Dyes Pigm.*, 2021, **187**, 109081.

24 Z. Xiang, Z.-Y. Wang, T.-B. Ren, W. Xu, Y.-P. Liu, X.-X. Zhang, P. Wu, L. Yuan and X.-B. Zhang, A general strategy for development of a single benzene fluorophore with full-color-tunable, environmentally insensitive, and two-photon solid-state emission, *Chem. Commun.*, 2019, **55**(76), 11462–11465.

25 X.-L. Peng, S. Ruiz-Barragan, Z.-S. Li, Q.-S. Li and L. Blancafort, Restricted access to a conical intersection to explain aggregation induced emission in dimethyl tetraphenylsilole, *J. Mater. Chem. C*, 2016, **4**(14), 2802–2810.

26 (*a*) J. Massue, A. Felouat, M. Curtil, P. M. Vérité, D. Jacquemin and G. Ulrich, Solution and Solid-State Excited-State Intramolecular Proton Transfer (ESIPT) emitters incorporating Bis-triethyl-or triphenylsilylethynyl units, *Dyes Pigm.*, 2019, **160**, 915–922; (*b*) T. Pariat, M. Munch, M. Durko-Maciag, J. Mysliwiec, P. Retailleau, P. M. Vérité, D. Jacquemin, J. Massue and G. Ulrich, Impact of Heteroatom Substitution on Dual-State Emissive Rigidified 2-(2′-hydroxyphenyl)benzazole Dyes: Towards Ultra-Bright ESIPT Fluorophores, *Chem. – Eur. J.*, 2021, **27**(10), 3483–3495.

27 T. Pariat, T. Stoerkler, C. Diguet, A. D. Laurent, D. Jacquemin, G. Ulrich and J. Massue, Dual Solution-/Solid-State Emissive Excited-State Intramolecular Proton Transfer (ESIPT) Dyes: A Combined Experimental and Theoretical Approach, *J. Org. Chem.*, 2021, **86**, 17606–17619.

28 T. Stoerkler, A. D. Laurent, G. Ulrich, D. Jacquemin and J. Massue, Influence of ethynyl extension on the dual-state emission properties of pyridinium-substituted ESIPT fluorophores, *Dyes Pigm.*, 2022, **208**, 110872.

29 D. Göbel, P. Rusch, D. Duvinage, T. Stauch, N. C. Bigall and B. J. Nachtsheim, Substitution Effect on 2-(Oxazolinyl)-phenols and 1,2,5-Chalcogenadiazole-Annulated Derivatives: Emission-Color-Tunable, Minimalistic Excited-State Intramolecular Proton Transfer (ESIPT)-Based Luminophores, *J. Org. Chem.*, 2021, **86**, 14333–14355.

30 D. Göbel, D. Duvinage, T. Stauch and B. J. Nachtsheim, Nitrile-substituted 2-(oxazolinyl)-phenols: minimalistic excited-state intramolecular proton transfer (ESIPT)-based fluorophores, *J. Mater. Chem. C*, 2020, **8**, 9213–9225.

31 K. Benelhadj, J. Massue, P. Retailleau, G. Ulrich and R. Ziessel, v2-(2′-Hydroxyphenyl)benzimidazole and 9,10-Phenanthroimidazole Chelates and Borate Complexes: Solution- and Solid-State Emitters, *Org. Lett.*, 2013, **15**, 2918–2921.

32 K. Takagi, Y. Yamada, R. Fukuda, M. Ehara and D. Takeuchi, ESIPT emission behavior of methoxy-substituted 2-hydroxyphenylbenzimidazole isomers, *New J. Chem.*, 2018, **42**(8), 5923–5928.

33 K. Takagi, K. Ito, Y. Yamada, T. Nakashima, R. Fukuda, M. Ehara and H. Masu, Synthesis and Optical Properties of Excited-State Intramolecular Proton Transfer Active π-Conjugated Benzimidazole Compounds: Influence of Structural Rigidification by Ring Fusion, *J. Org. Chem.*, 2017, **82**, 12173–12180.

34 J. Tian, D. Shi, Y. Zhang, X. Li, X. Li, H. Teng, T. D. James, J. Li and Y. Guo, Stress response decay with aging visualized using a dual-channel logic-based fluorescent probe, *Chem. Sci.*, 2021, **12**(40), 13483–13491.

35 I. Kaur, Shivani, P. Kaur and K. Singh, 2-(2′-Hydroxyphenyl)benzothiazole derivatives: Emission and color tuning, *Dyes Pigm.*, 2020, **176**, 108198.

36 M. Huang, J. Zhou, K. Xu, X. Zhu and Y. Wan, Enhancement of the excited-state intramolecular proton transfer process to produce all-powerful DSE molecules for bridging the gap between ACQ and AIE, *Dyes Pigm.*, 2019, **160**, 839–847.

37 V. Trannoy, A. Léaustic, S. Gadan, R. Guillot, C. Allain, G. Clavier, S. Mazerat, B. Geffroy and P. A. Yu, A highly efficient solution and solid state ESIPT fluorophore and its OLED application, *New J. Chem.*, 2021, **45**, 3014–3021.

38 C. C. Anghel, C. Badescu, A. G. Mirea, A. Paun, N. D. Nadade, A. M. Madalan, M. Matache and C. C. Popescu, Two are better than one - Synthesis of novel blue and green emissive hydroxy-oxadiazoles, *Dyes Pigm.*, 2022, **197**, 109927.

39 G. Xia, Q. Shao, K. Liang, Y. Wang, L. Jiang and H. Wang, A phenyl-removal strategy for accessing an efficient dual-state emitter in the red/NIR region guided by TDDFT calculations, *J. Mater. Chem. C*, 2020, **8**, 13621–13626.

40 J. Jankowska and A. L. Sobolewski, Modern Theoretical Approaches to Modeling the Excited-State Intramolecular Proton Transfer: An Overview, *Molecules*, 2021, **26**, 5140.

41 J. Tomasi, B. Mennucci and R. Cammi, Quantum Mechanical Continuum Solvation Models, *Chem. Rev.*, 2005, **105**, 2999–3094.

42 (*a*) M. Caricato, Absorption and Emission Spectra of Solvated Molecules with the EOM-CCSD-PCM Method, *J. Chem. Theory Comput.*, 2012, **8**, 4494–4502; (*b*) B. Lunkenheimer and A. Köhn, Solvent Effects on Electronically Excited States Using the Conductor-Like Screening Model and the Second-Order Correlated Method ADC(2), *J. Chem. Theory Comput.*, 2013, **9**, 977–994; (*c*) J. M. Mewes, J. M. Herbert and A. Dreuw, On the Accuracy of the General, State-Specific Polarizable-Continuum Model for the Description of Correlated Ground- and Excited States In Solution, *Phys. Chem. Chem. Phys.*, 2017, **19**, 1644–1654; (*d*) I. Duchemin, D. Jacquemin and X. Blase, Combining the GW Formalism with the Polarizable Continuum Model: A State-Specific Non-Equilibrium Approach, *J. Chem. Phys.*, 2016, **144**, 164106; (*e*) I. Duchemin, C. A. Guido, D. Jacquemin and X. Blase, The Bethe-Salpeter formalism with polarizable continuum embedding: reconciling linear-response and state-specific features, *Chem. Sci.*, 2018, **9**, 4430–4443.

43 C. A. Guido and S. Caprasecca, On the Description of the Environment Polarization Response to Electronic Transitions, *Int. J. Quantum Chem.*, 2019, **119**, e25711.

44 R. Cammi and B. Mennucci, Linear response theory for the polarizable continuum model, *J. Chem. Phys.*, 1999, **110**, 9877–9886.

45 M. Caricato, B. Mennucci, J. Tomasi, F. Ingrosso, R. Cammi, S. Corni and G. Scalmani, Formation and Relaxation of Excited States in Solution: A new Time Dependent Polarizable Continuum Model Based on Time Dependent Density Functional Theory, *J. Chem. Phys.*, 2006, **124**, 124520.

46 (*a*) P. M. Vérité, C. A. Guido and D. Jacquemin, First-principles investigation of the double ESIPT process in a thiophene-based dye, *Phys. Chem. Chem. Phys.*, 2019, **21**, 2307–2317; (*b*) C. A. Guido, A. Chrayteh, G. Scalmani, B. Mennucci and D. Jacquemin, Simple Protocol for Capturing Both Linear-Responseand State-Specific Effects in Excited-State Calculations with Continuum Solvation Models, *J. Chem. Theory Comput.*, 2021, **17**, 5155–5164.

47 M. Nottoli, M. Bondanza, F. Lipparini and B. Mennucci, An enhanced sampling QM/AMOEBA approach: The case of the excited state intramolecular proton transfer in solvated 3-hydroxyflavone, *J. Chem. Phys.*, 2021, **154**, 184107.

48 (*a*) J. Paterson, M. A. Robb, L. Blancafort and A. D. DeBellis, Theoretical Study of Benzotriazole UV Photostability: Ultrafast Deactivation through Coupled Proton and Electron Transfer Triggered by a Charge-Transfer State, *J. Am. Chem. Soc.*, 2004, **126**, 2912–2922; (*b*) J. Paterson, M. A. Robb, L. Blancafort and A. D. DeBellis, Mechanism of an Exceptional Class of Photostabilizers: A Seam of Conical Intersection Parallel to Excited State Intramolecular Proton Transfer (ESIPT) in o-Hydroxyphenyl-(1,3,5)-triazine, *J. Phys. Chem. A*, 2005, **109**, 7527–7537; (*c*) H. H. G. Tsai, H. L. S. Sun and C.-J. Tan, TD-DFT Study of the Excited-State Potential Energy Surfaces of 2-(2′-Hydroxyphenyl) benzimidazole and its Amino Derivatives, *J. Phys. Chem. A*, 2010, **114**, 4065–4079.

49 (*a*) D. Presti, F. Labat, A. Pedone, M. J. Frisch, H. P. Hratchian, I. Ciofini, M. C. Menziani and C. Adamo, Modeling emission features of salicylidene aniline molecular crystals: A QM/QM′ approach, *J. Comput. Chem.*, 2016, **37**, 861–870; (*b*) D. Presti, A. Pedone, I. Ciofini, F. Labat, M. C. Menziani and C. Adamo, Optical properties of the dibenzothiazolylphenol molecular crystals through ONIOM calculations: the effect of the electrostatic embedding scheme, *Theor. Chim. Acta*, 2016, **135**, 86; (*c*) D. Presti, L. Wilbraham, C. Targa, F. Labat, A. Pedone, M. C. Menziani, I. Ciofini and C. Adamo, Understanding Aggregation-Induced Emission in Molecular Crystals: Insights from Theory, *J. Phys. Chem. C*, 2017, **121**, 5747–5752.

50 (*a*) M. Rivera, M. Dommett and R. Crespo-Otero, ONIOM(QM:QM′) electrostatic embedding schemes for photochemistry in molecular crystals, *J. Chem. Theory Comput.*, 2019, **15**, 2504–2516; (*b*) M. Rivera, M. Dommett, A. Sidat, W. Rahim and R. Crespo-Otero, Fromage: A library for the study of molecular crystal excited states at the aggregate scale, *J. Comput. Chem.*, 2020, **41**, 1045–1058; (*c*) M. Dommett, M. Rivera, M. T. H. Smith and R. Crespo-Otero, Molecular and crystalline requirements for solid state fluorescence exploiting excited state intramolecular proton transfer, *J. Mater. Chem. C*, 2020, **8**, 2558–2568.

51 (*a*) M. Dommett, M. Rivera and R. Crespo-Otero, How Inter- and Intramolecular Processes Dictate Aggregation-Induced Emission in Crystals Undergoing Excited-State Proton Transfer, *J. Phys. Chem. Lett.*, 2017, **8**, 6148–6153; (*b*) Q. Zhang, Y. Li, Z. Cao and C. Zhu, Aggregation-induced emission spectra of triphenylamine salicylaldehyde derivatives via excited-state intramolecular proton transfer revealed by molecular spectral and dynamics simulations, *RSC Adv.*, 2021, **11**, 37171–37180; (*c*) H. Wang, Q. Gong, G. Wang, J. Dang and F. Liu, Deciphering the Mechanism of Aggregation-Induced Emission of a Quinazolinone Derivative Displaying Excited-State Intramolecular Proton-Transfer Properties: A QM, QM/MM, and MD Study, *J. Chem. Theory Comput.*, 2019, **15**, 5440–5447; (*d*) J. Zhao, H. Dong, H. Yang and Y. Zheng, Aggregation Promotes Excited-State Intramolecular Proton Transfer for Benzothiazole-Substituted Tetraphenylethylene Compound, *ACS Appl. Bio Mater.*, 2019, **2**, 5182–5189.

52 O. Svelto, *Principles of lasers*, Springer, New York, 5th edn, 2010.

53 (*a*) J. A. Myer, I. Itzkan and E. Kierstead, Dye Lasers in the Ultraviolet, *Nature*, 1970, **225**(5232), 544–545; (*b*) P. Chou, D. McMorrow, T. J. Aartsma and M. Kasha, The Proton-Transfer Laser. Gain Spectrum and Amplification of Spontaneous Emission of 3-Hydroxyflavone, *J. Phys. Chem.*, 1984, **88**(20), 4596–4599.

54 J. Massue, T. Pariat, P. M. Vérité, D. Jacquemin, M. Durko, T. Chtouki, L. Sznitko, J. Mysliwiec and G. Ulrich, Natural Born Laser Dyes: Excited-State Intramolecular Proton Transfer (ESIPT) Emitters and Their Use in Random Lasing Studies, *Nanomaterials*, 2019, **9**(8), 1093.

55 C.-C. Yan, X.-D. Wang and L.-S. Liao, Organic Lasers Harnessing Excited State Intramolecular Proton Transfer Process, *ACS Photonics*, 2020, **7**(6), 1355–1366.

56 D. Gormin, A. Sytnik and M. Kasha, Spectroscopy of Amplified Spontaneous Emission Laser Spikes in Polyhydroxyflavones, *J. Phys. Chem. A*, 1997, **101**(4), 672–677.

57 D. A. Arthenopoulos, D. P. McMorrow and M. Kasha, Comparative Study of Stimulated Proton-Transfer Luminescence of Three Chromones, *J. Phys. Chem.*, 1991, **95**(7), 2668–2674.

58 P.-T. Chou, M. L. Martinez and J. H. Clements, The Observation of Solvent-Dependent Proton-Transfer/Charge-Transfer Lasers from 4′-Diethylamino-3-Hydroxyflavone, *Chem. Phys. Lett.*, 1993, **204**(5–6), 395–399.

59 A. U. Acuña, F. Amat, J. Catalán, A. Costela, J. M. Figuera and J. M. Muñoz, Pulsed Liquid Lasers from Proton Transfer in the Excited State, *Chem. Phys. Lett.*, 1986, **132**(6), 567–569.

60 A. U. Acuña, A. Costela, J. M. Muñoz and A. Proton-Transfer, Laser, *J. Phys. Chem.*, 1986, **90**(13), 2807–2808.

61 S. Park, O.-H. Kwon, S. Kim, S. Park, M.-G. Choi, M. Cha, S. Y. Park and D.-J. Jang, Imidazole-Based Excited-State Intramolecular Proton-Transfer Materials: Synthesis and Amplified Spontaneous Emission from a Large Single Crystal, *J. Am. Chem. Soc.*, 2005, **127**(28), 10070–10074.

62 H. H. Lim, S. Boomadevi, O.-Y. Jeon, K. Kyhm, M. Cha, S. Park and S. Y. Park, Polarization-Dependent Optical Gain in Crystal and Glass Composed of Excited-State Intramolecular Proton Transfer Organic Molecules, *Mater. Lett.*, 2007, **61**(19–20), 4213–4215.

63 L. Chen, S.-Y. Yin, M. Pan, K. Wu, H.-P. Wang, Y.-N. Fan and C.-Y. Su, A Naked Eye Colorimetric Sensor for Alcohol Vapor Discrimination and Amplified Spontaneous Emission (ASE) from a Highly Fluorescent Excited-State Intramolecular Proton Transfer (ESIPT) Molecule, *J. Mater. Chem. C*, 2016, **4**(29), 6962–6966.

64 X. Wang, Q. Liao, X. Lu, H. Li, Z. Xu and H. Fu, Shape-Engineering of Self-Assembled Organic Single Microcrystal as Optical Microresonator for Laser Applications, *Sci. Rep.*, 2014, **4**(1), 1–8.

65 J. Li, Y. Wu, Z. Xu, Q. Liao, H. Zhang, Y. Zhang, L. Xiao, J. Yao and H. Fu, Tuning the Organic Microcrystal Laser Wavelength of ESIPT-Active Compounds *via* Controlling the Excited Enol* and Keto* Emissions, *J. Mater. Chem. C*, 2017, **5**(46), 12235–12240.

66 X. Cheng, K. Wang, S. Huang, H. Zhang, H. Zhang and Y. Wang, Organic Crystals with Near-Infrared Amplified Spontaneous Emissions Based on 2′-Hydroxychalcone Derivatives: Subtle Structure Modification but Great Property Change, *Angew. Chem. Int. Ed.*, 2015, **54**(29), 8369–8373.

67 (*a*) J. Massue, A. Felouat, P. M. Vérité, D. Jacquemin, K. Cyprych, M. Durko, L. Sznitko, J. Mysliwiec and G. Ulrich, An Extended Excited-State Intramolecular Proton Transfer (ESIPT) Emitter for Random Lasing Applications, *Phys. Chem. Chem. Phys.*, 2018, **20**(30), 19958–19963; (*b*) M. Durko-Maciag, D. Jacquemin, G. Ulrich, J. Massue and J. Mysliwiec., Color-Tunable Multifunctional Excited-State Intramolecular Proton Transfer Emitter: Stimulated Emission of a Single Dye, *Chem. – Eur. J.*, 2022, **28**(44), e202201327.

68 C. E. Fellows, U. Tauber, C. C. Rodegheri, C. E. M. Carvalho, F. D. Acevedo, S. G. Bertolotti and C. Barbero, ASE and Photodegradation of Two Benzimidazole Derivatives Proton Transfer Dyes in Polymeric Matrices, *Opt. Mater.*, 2004, **27**(3), 499–502.

69 W. Zhang, Y. Yan, J. Gu, J. Yao and Y. S. Zhao, Low-Threshold Wavelength-Switchable Organic Nanowire Lasers Based on Excited-State Intramolecular Proton Transfer, *Angew. Chem. Int. Ed.*, 2015, **54**(24), 7125–7129.

70 A. U. Acuña, F. Amat-Guerri, A. Costela, A. Douhal, J. M. Figuera, F. Florido and R. Sastre, Proton-Transfer Lasing from Solid Organic Matrices, *Chem. Phys. Lett.*, 1991, **187**(1), 98–102.

71 S. Park, J. E. Kwon, S.-Y. Park, O.-H. Kwon, J. K. Kim, S.-J. Yoon, J. W. Chung, D. R. Whang, S. K. Park, D. K. Lee, D.-J. Jang, J. Gierschner and S. Y. Park., Crystallization-Induced Emission Enhancement and Amplified Spontaneous Emission from a CF_3-Containing Excited-State Intramolecular-Proton-Transfer Molecule, *Adv. Opt. Mater.*, 2017, **5**(18), 1700353.

72 J. Wu, M. Zhuo, R. Lai, S. Zou, C. Yan, Y. Yuan, S. Yang, G. Wei, X. Wang and L. Liao, Cascaded Excited-State Intramolecular Proton Transfer Towards Near-Infrared Organic Lasers Beyond 850 nm, *Angew. Chem., Int. Ed.*, 2021, **60**(16), 9114–9119.

73 J. E. Kwon and S. Y. Park, Advanced Organic Optoelectronic Materials: Harnessing Excited-State Intramolecular Proton Transfer (ESIPT) Process, *Adv. Mater.*, 2011, **23**(32), 3615–3642.

74 P. Zhou and K. Han, ESIPT-Based AIE Luminogens: Design Strategies, Applications, and Mechanisms, *Aggregate*, 2022, **3**(5), e160.

75 H. Lin, X. Chang, D. Yan, W.-H. Fang and G. Cui, Tuning Excited-State-Intramolecular-Proton-Transfer (ESIPT) Process and Emission by Cocrystal Formation: A Combined Experimental and Theoretical Study, *Chem. Sci.*, 2017, **8**(3), 2086–2090.

76 M. Chu, B. Qiu, W. Zhang, Z. Zhou, X. Yang, Y. Yan, J. Yao, Y. Li and Y. S. Zhao, Tailoring the Energy Levels and Cavity Structures toward Organic Cocrystal Microlasers, *ACS Appl. Mater. Interfaces*, 2018, **10**(49), 42740–42746.

77 Y. Tsutsui, W. Zhang, S. Ghosh, T. Sakurai, H. Yoshida, M. Ozaki, T. Akutagawa and S. Seki, Electrically Switchable Amplified Spontaneous Emission from Liquid Crystalline Phase of an AIEE-Active ESIPT Molecule, *Adv. Opt. Mater.*, 2020, **8**(14), 1902158.

78 Y. Geng, Y. Zhao, Y. Zhao, F. Feng, J. Zhang, X. Fan, H. Gao, X.-D. Wang, L. Jiang and Y. Wu, Multifunctional Organic Single-Crystalline Microwire Arrays toward Optical Applications, *Adv. Funct. Mater.*, 2022, **32**(19), 2113025.

79 G.-Q. Wei, Y. Yu, M.-P. Zhuo, X.-D. Wang and L. S. Liao, Organic Single-Crystalline Whispering-Gallery Mode Microlasers with Efficient Optical Gain Activated via Excited State Intramolecular Proton Transfer Luminogens, *J. Mater. Chem. C*, 2020, **8**(34), 11916–11921.

80 X. Cheng, Y. Zhang, S. Han, F. Li, H. Zhang and Y. Wang, Multicolor Amplified Spontaneous Emissions Based on Organic Polymorphs That Undergo Excited-State Intramolecular Proton Transfer, *Chem. – Eur. J.*, 2016, **22**(14), 4899–4903.

81 H. Dong, C. Zhang, J. Yao and Y. S. Zhao, Wavelength-Controlled Organic Microlasers Based on Polymorphism-Dependent Intramolecular Charge-Transfer Process, *Chem. – Asian J.*, 2016, **11**(19), 2656–2661.

82 X. Wang, Z.-Z. Li, S.-F. Li, H. Li, J. Chen, Y. Wu and H. Fu., Near-Infrared Organic Single-Crystal Lasers with Polymorphism-Dependent Excited State Intramolecular Proton Transfer, *Adv. Opt. Mater.*, 2017, **5**(12), 1700027.